Polymer Bulletin 38, 469–476 (1997)

Polymer Bulletin

Small-angle X-ray scattering with imaging plate

Application to dilute polymer solutions

Yo Nakamura[1,*], **Katsumi Akashi**[1], **Takashi Norisuye**[1], **Akio Teramoto**[1], **Mamoru Sato**[2]

[1] Department of Macromolecular Science, Osaka University, Toyonaka, Osaka 560, Japan
[2] Institute for Protein Research, Osaka University, Suita, Osaka 565, Japan

Received: 2 December 1996/Revised version: 26 December 1996/Accepted: 27 December 1996

Summary

A new small-angle X-ray scattering apparatus with a pinhole slit collimation camera and an imaging plate detector was constructed and tested with two polystyrene samples of molecular weights 1×10^4 and 2×10^4 in cyclohexane at 34.5°C (the theta point) and toluene at 15°C and also with aqueous aurous colloids. This apparatus requires no desmearing procedure. Its usefulness for polymer solution studies is demonstrated by the measured radii of gyration and scattering functions.

Introduction

In laboratory-scale measurements of small-angle X-ray scattering (SAXS) from dilute polymer solutions, apparatuses with a line-slit camera and a one-dimensional detector are usually used, and measured scattering intensities are corrected for the slit length effect by the desmearing procedure (1). This correction often requires undesirable smoothing of raw scattering intensity curves and does not always give the true scattering function at high scattering angles (2,3). Use of a pinhole slit collimation camera frees the desmearing problem, but it has been impractical with conventional X-ray sources owing to substantial reduction in incident beam intensity.

Recently it was found that the two-dimensional imaging plate (IP) detector developed for X-ray diffraction reduces to a great extent the measuring time in crystalline structure determination by virtue of its high sensitivity (4). This improvement on the detector system motivated us to construct an IP-SAXS apparatus with a pinhole collimation camera for polymer solution studies. We suspected that even with such a camera, the IP detector allows weak SAXS intensities from dilute polymer solutions to be measured with reasonable accuracy. This paper describes the apparatus constructed and some

* Corresponding author

results from SAXS measurements made on polystyrene solutions and aurous colloid suspensions to test it.

Experimental

Apparatus

The diagram of our SAXS apparatus is schematically shown in Figure 1. The X-ray beam from the copper rotating anode (A) of a Rigaku RU-200 X-ray generator (operated at 150 kV - 40 mA) is monochronized by a graphite plate (B) to extract the Kα line (wavelength $\lambda = 0.154$ nm), and narrowed by two pinhole slits (1 and 2, both with 0.2 mm diameter). Slit 3, whose pinhole size and position are adjustable, removes parasitic scattering from slit 2. All these slits are placed in the evacuated slit box (C). The beam scattered from the test solution in a quartz-glass capillary of 1.5 mm in diameter passes through the vacuum path (E) of 500 mm length and is detected by IP as a two-dimensional image, which is processed by an IP reading system (F) (Rigaku R-AXIS DS). Part of the beam is blocked off by a beam stopper (3 mm in width) at the end of the vacuum path. The available scattering angle ranges from 0.15 to 5°. The temperature of the solution is kept within ±0.05°C by circulation of temperature-regulated water through the capillary holder (D).

Measurement and Analysis

Our apparatus was tested with cyclohexane and toluene solutions of two narrow-distribution samples of atactic polystyrene (designated F1-B and 2b-B) and aqueous suspensions of aurous colloids (Polysciences, Inc.). The weight-average molecular weights M_w of samples F1-B and 2b-B were previously determined by light scattering to be 1.03×10^4 and 1.98×10^4, respectively (5). The commercially available colloidal gold suspension (0.01% concentration) was concentrated to 0.05% before use. SAXS data for all these test samples were accumulated for 8h.

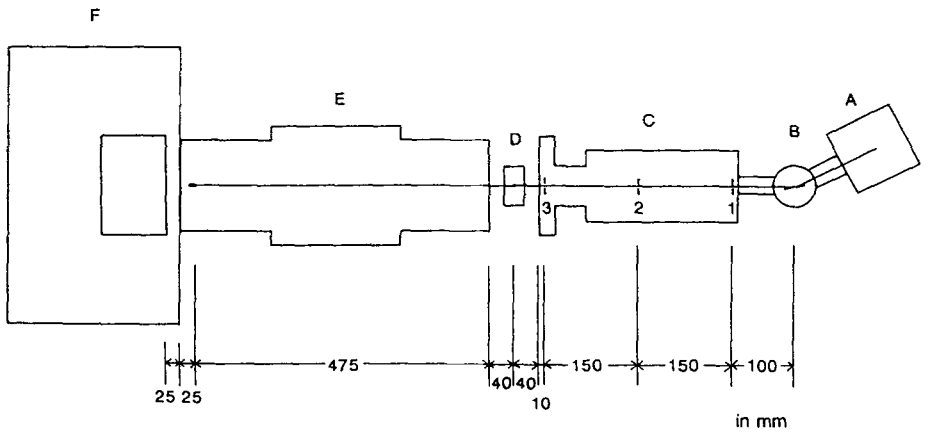

Figure 1. Schematic diagram of the small-angle X-ray scattering apparatus constructed: A, X-ray generator; B, graphite monochromator; C, slit box; D, capillary holder; E, vacuum path; F, imaging plate (IP) and IP reading system.

Figure 2A shows by way of example the scattering image obtained for the cyclohexane solution of polystyrene sample 2b-B with a polymer mass concentration c of 8.64×10^{-2} g cm^{-3} at 34.5°C (the theta temperature). Note that the middle portion of the image is blocked off by the beam stopper. The darkness of the image, which is proportional to the scattering intensity, is digitized at intervals of 0.05 mm by the IP reading system. The scattering intensity at a scattering angle θ is then given by the sum of those values at the same radial distance from the beam center (indicated by the cross in Figure 2B). In actuality, however, it was obtained by collecting all data in an angular range from $\theta - \Delta\theta$ to $\theta + \Delta\theta$, i.e., within a pair of arched bands of width $2\Delta\theta$, with $\Delta\theta$ taken to be 0.005 - 0.04° (the case of $\Delta\theta = 0.02°$ is shown in the Figure 2B), and the resulting integrated intensity divided by the band area was taken as the desired scattering intensity I_θ at θ.

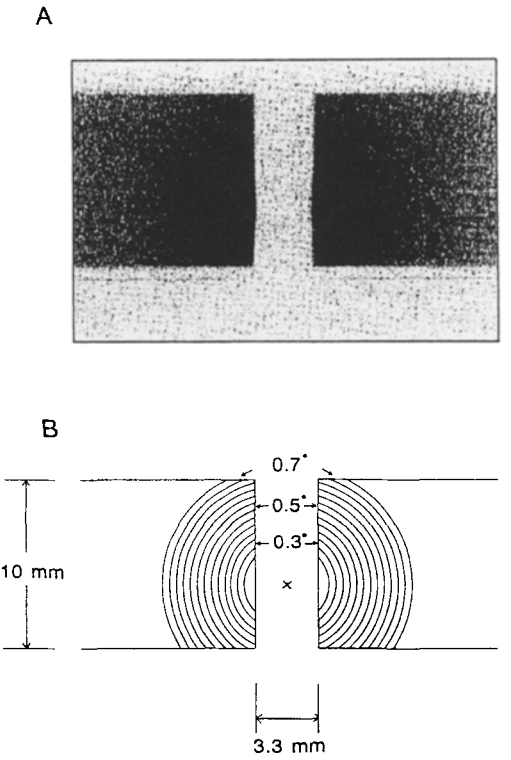

Figure 2. Scattering image from a cyclohexane solution ($c = 0.0864$ g cm^{-3}) of polystyrene sample 2b-B at 34.5°C (A) and its divisions at constant scattering angles (B). The cross indicates the beam center.

Apparently, a larger $\Delta\theta$ diminishes the scatter of data as a function of θ but may lead to less accurate I_θ because of the lowering in angular resolution. As explained below, $\Delta\theta$ values smaller than 0.042° introduce no substantial error in the radius of gyration $\langle S^2 \rangle^{1/2}$ and the particle scattering function $P(\theta)$ for relatively small particles with which SAXS measurements are usually concerned.

With the known expressions of $P(\theta)$ for Gaussian chains, thin rods, and rigid spheres, we computed the "experimental" scattering function $\tilde{P}(\theta)$ defined by

$$\tilde{P}(\theta) = \frac{1}{2\Delta\theta} \int_{\theta-\Delta\theta}^{\theta+\Delta\theta} P(\theta)\, d\theta \qquad (1)$$

The results showed that except for spheres at particular angles where $P(\theta) \approx 0$, the difference between $\tilde{P}(\theta)$ and $P(\theta)$ does not exceed 1% if $\Delta\theta\langle S^2\rangle^{1/2} < 7.35 \times 10^{-3}$ rad nm (i.e., if $\Delta\theta < 0.042^\circ$ for $\langle S^2\rangle^{1/2} < 10$ nm) for $\lambda = 0.154$ nm, and that under this condition, the radius of gyration derived from $\tilde{P}(\theta)$ does not differ more than 1% from the true value. For spheres, the relative deviation of $\tilde{P}(\theta)$ from $P(\theta)$ becomes exceptionally large (10 - 100%) when $P(\theta)$ decreases below 0.01. However, those errors are insignificant in that the difference $\tilde{P}(\theta) - P(\theta)$ stays less than 0.005.

The solvent intensity was measured before and after the measurement on every solution and its mean was subtracted from the intensity for the solution to obtain the excess scattering intensity ΔI_θ at θ. The intensity of incident beam was monitored by measuring the scattering intensity for a thin polyethylene film (1 mm thickness) placed just behind the capillary, but its correction for fluctuation happened to be unnecessary in the present data given below.

Results and Discussion

Aurous Colloid Suspension

We first examined the reproducibility of ΔI_θ using an aurous colloid suspension at a single concentration of 0.05%. The results obtained for $\Delta\theta = 0.02^\circ$ are displayed in Figure 3, in which ΔI_0 is the value of ΔI_θ extrapolated to $\theta = 0$ by the square-root plot and k is the magnitude of the scattering vector defined by $k = (4\pi/\lambda)\sin(\theta/2)$. The two sets of independently measured $\Delta I_\theta/\Delta I_0$ distinguished by different symbols are seen to fall essentially on a single curve, thus showing that our measurements were reproducible.

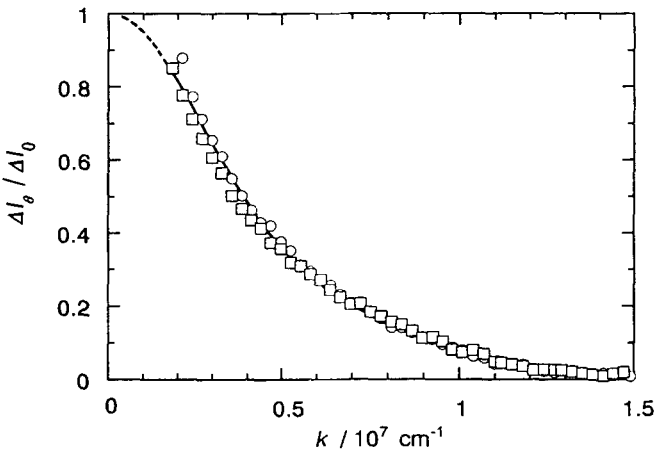

Figure 3. Angular dependence of scattering function $\Delta I_\theta/\Delta I_0$ for an aqueous aurous colloid suspension with a concentration of 0.05 %. Different symbols, independent measurements.

Polystyrene

Figure 4 illustrates the angular dependence of $(c/\Delta I_\theta)^{1/2}$ for polystyrene sample 2b-B in cyclohexane at 34.5°C, derived from the scattering image ($\Delta\theta = 0.005°$) in Figure 2A. The data points for $k^2 < 1.5 \times 10^{13}$ cm^{-2} are fitted by a straight line, whose slope S and intercept I give the apparent z-average mean-square radius of gyration $\langle S^2\rangle_{z,app}$ [$\equiv 6(S/I)$].

The concentration dependence of $\langle S^2\rangle_{z,app}^{1/2}$ for the two polystyrene samples in cyclohexane at the theta temperature is shown in Figure 5. The data points for either sample follow a horizontal line, whose height is equated to $\langle S^2\rangle_z^{1/2}$ (the z-average $\langle S^2\rangle^{1/2}$) at $c = 0$.

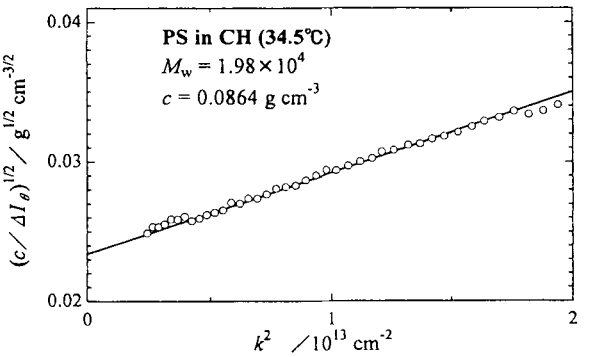

Figure 4. Angular dependence of $(c/\Delta I_\theta)^{1/2}$ for polystyrene sample 2b-B in cyclohexane at 34.5°C.

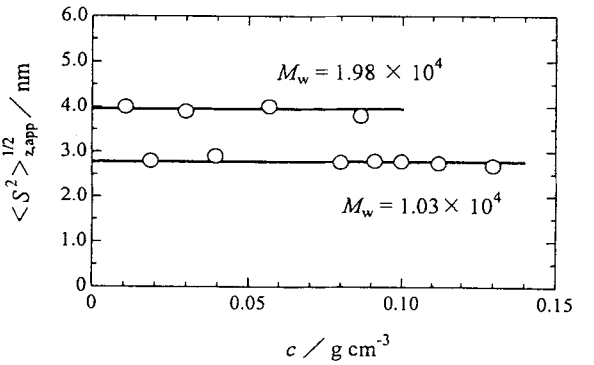

Figure 5. Concentration dependence of $\langle S^2\rangle_{z,app}^{1/2}$ for two polystyrene samples in cyclohexane at 34.5°C.

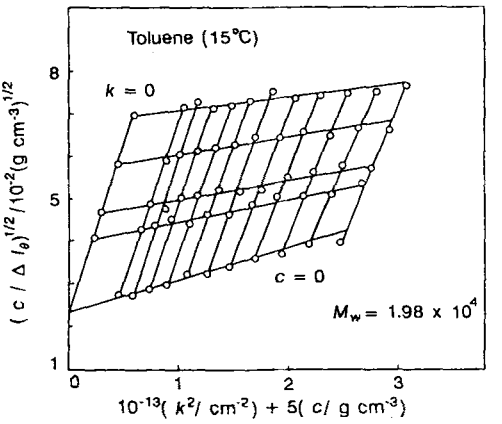

Figure 6. Zimm plot in the square-root form for polystyrene sample 2b-B in toluene at 15°C.

The scattering data for the two samples in toluene at 15°C were similarly analyzed, but the extrapolation of $\langle S^2 \rangle_{z,app}^{1/2}$ to $c = 0$ was difficult because $\langle S^2 \rangle_{z,app}^{1/2}$ in this good solvent depended strongly on c. Thus, the data were analyzed by the Zimm plot in the square-root form, as illustrated in Figure 6.

The values of $\langle S^2 \rangle_z^{1/2}$ for F1-B and 2b-B in the two solvents are summarized in Table I, along with the literature data (6,7) obtained for samples of similar molecular weights with a Kratky U-slit camera and by desmearing of intensities. Our data are seen to agree with the literature values within ±2%. The second virial coefficients A_2 for samples F1-B and 2b-B in toluene at 15°C were 12×10^{-4} and 8.4×10^{-4} cm^3 mol g^{-2}, respectively, when estimated with the aid of M_w. The latter A_2 value is also in substantial agreement with the literature value (8.8×10^{-4} cm^3 mol g^{-2}) for $M_w = 2.05 \times 10^4$ (7).

Table I Radii of Gyration for Polystyrene Samples from SAXS Measurements

$10^{-4} M_w$	$\langle S^2 \rangle_z^{1/2}$ / nm	
	in Cyclohexane (34.5°C)	in Toluene (15°C)
1.03	2.8	2.9
1.01[a]	2.75	2.95
1.98	4.0	4.4
2.05[b]	3.98	4.34

[a] ref. 6, [b] ref. 7

The unfilled circles in Figure 7 show the Kratky plot of $F(k)$ vs. k (at $c \rightarrow 0$) for sample F1-B in cyclohexane at 34.5°C, where $F(k)$ is defined by

$$F(k) = k^2 M_w P(\theta) \qquad (2)$$

The filled circles represent the data for $M_w = 1.01 \times 10^4$ reported by Koyama et al.(8), who used a point-focusing camera with a high intensity generator at the High-Intensity X-ray Laboratory of Kyoto University. The agreement between the two data sets is very satisfactory.

In short, the present SAXS data for an aurous colloid suspension and polystyrene solutions are reliable (or at least reproducible) with respect to the concentration and angular dependences of intensity. This demonstrates the usefulness of our new IP-SAXS apparatus for polymer solution studies.

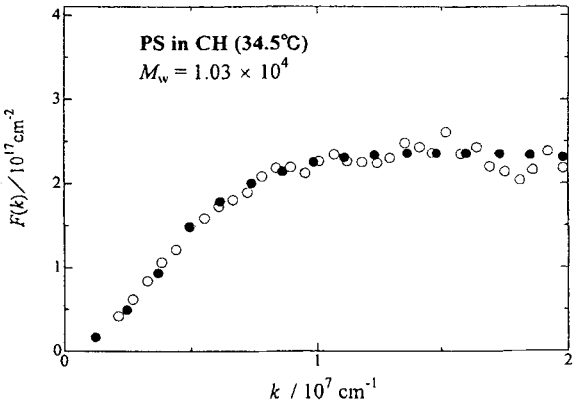

Figure 7. Kratky plot for polystyrene sample F1-B in cyclohexane at 34.5°C. (○), present data for $\Delta\theta = 0.04°$; (●), Koyama et al.(ref. 8).

Acknowledgment

This work was supported by a Grant-in-Aid for Scientific Research (No. 06403027) from the Ministry of Education, Science, Sports and Culture of Japan.

References

1. Glatter O, Kratky O (1982) *Small Angle X-ray Scattering*, Academic Press, London.
2. Yoshizaki T, Hayashi H, Yamakawa H (1993) *Macromolecules* **26**: 4037.
3. Yoshizaki T, Hayashi H, Yamakawa H (1994) *Macromolecules* **27**: 4259.
4. Sato M, Yamamoto M, Imada K, Katsube Y, Tanaka N, Higashi T (1992) *J. Appl. Cryst.* **25**: 348.

5. Nakamura Y, Norisuye T, Teramoto A (1991) *J. Polym. Sci.: Part B: Polym. Phys.* **29**: 153.
6. Konishi T, Yoshizaki T, Saito T, Einaga Y, Yamakawa H (1990) *Macromolecules* **23**: 290.
7. Abe F, Einaga Y, Yoshizaki T, Yamakawa H (1993) *Macromolecules* **26**: 1884.
8. Koyama H, Yoshizaki T, Einaga Y, Hayashi H, Yamakawa H (1991) *Macromolecules* **24**: 932 .